

# THE LANCET

## Infectious Diseases

### Supplementary appendix

This appendix formed part of the original submission and has been peer reviewed.  
We post it as supplied by the authors.

Supplement to: Sheward DJ, Kim C, Ehling RA, et al. Neutralisation sensitivity of the SARS-CoV-2 omicron (B.1.1.529) variant: a cross-sectional study. *Lancet Infect Dis* 2022; published online March 17. [https://doi.org/10.1016/S1473-3099\(22\)00129-3](https://doi.org/10.1016/S1473-3099(22)00129-3).

## **Supplementary Material**

### **Supplementary Methods**

1. Cloning Strategy. **Page 2.**
2. Monoclonal Antibody Production. **Page 3.**
3. AlphaFold2 Omicron Model. **Page 4.**
4. Monoclonal Antibody Escape Mutations. **Page 4.**

### **Supplementary Figures**

- Supplementary Figure 1. Cloning strategy. **Page 5.**
- Supplementary Figure 2. Neutralization curves. **Page 6.**
- Supplementary Figure 3. Neutralizing activity compared to Delta. **Page 7.**
- Supplementary Figure 4. Neutralizing activity compared to Beta and Mu. **Page 7.**
- Supplementary Figure 5. Correlations. **Page 8.**

### **Supplementary Tables**

- Supplementary Table 1. List of mutations in the Omicron spike evaluated here, relative to Wu-Hu-1. **Page 9.**
- Supplementary Table 2. Neutralizing ID<sub>50</sub> titers for pooled vaccine standard reagents. **Page 9.**
- Supplementary Table 3. Heterogeneity in fold-changes. **Page 10.**

**References. Page 11.**

## **Supplementary Methods**

### **1. Cloning Strategy**

RNA from a patient sample was isolated using a GeneJet Viral RNA extraction kit (ThermoFisher Scientific), and cDNA was generated using Superscript IV (Invitrogen) using Random Hexamer primers, per the manufacturers' instructions. An amplicon encompassing the entire spike was first amplified from cDNA using Q5 High Fidelity 2x Master Mix (New England Biolabs), and a second-round PCR was used to amplify a sub-region of the spike (with codons corresponding to amino acid positions 43 to 1000) incorporating all of the Omicron variant reference mutations. This second round also introduced Gibson assembly overhangs, exploiting regions of existing homology between the codon-optimized parent plasmid and the codon-native spike, in order to maximize overhang length while still keeping primer length under 35bp, allowing for overnight primer synthesis. The N-terminal and C-terminal flanking regions of the parent plasmid were similarly amplified. The three PCR products were cloned by Gibson Assembly into a restriction-enzyme (NheI and XbaI) digested, codon-optimized SARS-CoV-2 Spike expression vector (in pcDNA3.1) harbouring a mutation that introduces a stop codon that truncates the last 19 amino acids of the cytoplasmic tail (facilitating efficient incorporation onto lentiviral particles). The resulting spike-encoding expression vector was confirmed by sequencing to encode an amino acid sequence identical to that of the Omicron consensus. A visual depiction of the cloning strategy is available in Supplementary Figure 1.

### **Primers (5'-3')**

#### **Spike PCR:**

##### First round (primers from <sup>1</sup>):

SARSCoV1200\_22\_LEFT GTGATGTTCTTGTTAACAACAACTAAACGAACA

SARSCoV1200\_24\_RIGHT ATGAGGTGCTGACTGAGGGAAG

##### Second round:

FWD\_N\_term\_sample CAAGGTGTTTCAGATCCTCAGTTTTACATTCAACTC

REV\_C\_term\_sample TCTGCAGTCTGCCTGTGATCAACCTATCAATTTGC

#### **N-terminus flank PCR:**

Fwd\_CMV\_plasmid ACGCAAATGGGCGGTAGGCGTG

REV\_N\_term\_plasmid TGAATGTAAAACCTGAGGATCTGAACACCTTGTCGG

#### **C-terminus flank PCR:**

FWD\_C\_term\_plasmid AAATTGATAGGTTGATCACAGGCAGACTGCAGAGC

Rev\_plasmid TGGCAACTAGAAGGCACAGTCGAG

## Cloned Omicron Spike coding sequence (with 19AA CT truncation)

Native codon Omicron insert Codon optimized parent sequence (no AA differences to Omicron reference)

```
ATGTTCTGTTTCTGGTGTCTGCTGCCTCTGGTGTCCAGCCAGTGTGTGAACCTGACCACCAGAACACAGCTGCCTCCAGCCTACAC
CAACAGCTTTACCAGAGGCGTGTACTACCCCGACAAGGTGTTTCAGATCCTCAGTTTACATTCAACTCAGGACTTGTCTTACCTTT
CTTTTCCAATGTTACTTGGTTCATGTTATCTCTGGGACCAATGGTACTAAGAGGTTTGATAACCCTGTCTACCATTTAATGATGG
TGTTTATTTTGGCTTCCATTGAGAAGTCTAACATAATAAGAGGCTGGATTTTGGTACTACTTTAGATTGGAAGCCAGTCCCTACT
TATTGTAAATAACGCTACTAATGTTGTTATTAAGTCTGTGAATTTCAATTTTGAATGATCCATTTTGGACCACAAAAACAACAA
AAGTTGGATGGAAGTGAGTTCAGAGTTTATTCTAGTGCGAATAATTGCACTTTTGAATATGTCTCTCAGCCTTTCTTATGGACCT
TGAAGGAAAACAGGGTAATTTCAAAAAATCTTAGGGAATTTGTGTTAAGAATATTGATGGTTATTTAAAAATATATTCTAAGCACA
CGCCTATTATAGTGTGAGCCAGAAGATCTCCCTCAGGGTTTTTCGGCTTTAGAACCATTTGGTAGATTGGCAATAGGTATTAAC
ATCACTAGGTTTCAAACTTTACTTGTCTTACATAGAAAGTTATTTGACTCTGGTGTATTCTTCTCAGGTTGGACAGCTGGTGTGCA
GCTTATTATGTGGGTTATCTCAACCTAGGACTTTTCTATTAATAATAATGAAAAATGGAACCATTACAGATGTCTGAGACTGTGC
ACTTGACCCTCTCTCAGAAACAAAGTGTACGTTGAAATCCTTCACTGTAGAAAAAGGAATCTATCAAACCTTCTAACTTTAGAGTCC
AACCAACAGAATCTATTGTTAGATTTCTAATATTACAAACTGTGCCCTTTGATGAAGTTTAAACGCCACCAGATTTGCATCTG
TTATGTCTGGAAACAGGAAGAGAATCAGCAACTGTGTGCTGATTATTTCTGTCCTATATAATCTCGCACCATTTTCACTTTAAGT
GTTATGGAGTGTCTCTACTAAATTAATGATCTCTGCTTACTAATGTCTATGCAGATTCATTTGTAATTAGAGGTGATGAAGTCA
GACAAATCGCTCCAGGGCAAACCTGGAATATTGCTGATTATAATTATAAATACCAGATGATTTTACAGGCTGCGTTATAGCTTGG
AATTCTAACAAAGCTTGATTCTAAGGTTAGTGGTAATTATAATTACCTGTATAGATTGTTTAGGAAGTCTAATCTCAAACCTTTTGA
GAGAGATATTTCAACTGAAATCTATCAGGCCGGTAACAACTTGTAAATGGTGTGCAGGTTTAAATTGTTACTTTCTTTACGAT
CATATAGTTTCCGACCCACTTATGGTGTGGTCCCAACCATACAGAGTAGTAGTACTTTCTTTGAACTTCTACATGCACCAGCA
ACTGTTTGTGGACCTAAAAAGTCTACTAATTTGGTTAAAAACAATGTGTCAATTTCAACTTCAATGGTTTAAAGGCACAGGTGT
TCTTACTGAGTCTAACAAAAAGTTTCTGCCTTTCCAACAATTTGGCAGAGACATTGCTGACACTACTGATGTGTCCGTGATCCAC
AGACACTTGAGATCTTGACATTACACCATGTTCTTTGGTGGTGTCAAGTGTATAAACACCAGGAACAATACTCTAACCCAGGTT
GCTGTCTTTATCAGGGTGTAACTGCACAGAAGTCCCTGTTGCTATTCTATGCAGATCAACTTACTCTACTTGGCGTGTATTCT
ACAGGTTCTAATGTTTTCAAACACGTGCAGGCTGTTAATAGGGGCTGAATATGTCAACAACCTCATATGAGTGTGACATACCCAT
TGGTGCAGGTATATGCGCTAGTTATCAGACTCAGACTAAGTCTCATCGGCGGGCACGTAGTGTAGCTAGTCAATCCATCATTGCCT
ACACTATGTCACTTGGTGCAGAAAATTCAGTTGCTTACTCTAATAACTCTATTGCCATACCACAAAATTTTACTATTAGTGTACCA
CAGAAATCTACCAGTGTCTATGACCAAGACATCAGTAGATTGTACAATGTACATTTGTGGTGTATCACTGAATGCAGCAATCTT
TTGTTGCAATATGGCAGTTTTTGTACACAATTAACCGTGTCTTAACTGGAATAGCTGTTGAACAAGACAAAAACACCCAAGAAG
TTTTTGCACAAGTCAAAACAAATTTCAAAAAACACCACCAATTAATATTTTGGTGGTTTTAATTTTTCACAAATATTACCAGATCCAT
CAAAACCAAGCAAGAGGTCATTTATTGAAGATCTACTTTTCAACAAAGTGACACTTGCAGATGCTGGCTTCATCAAAACAATATGG
TGATTGCCTTGGTGATATTGCTGCTAGAGACCTCAATTTGTGCACAAAAGTTTAAAGGCCTTACTGTTTGGACCCTTGTCTCACAGA
TGAAATGATTGCTCAATACACTTCTGCACTGTTAGCGGTACAATCACTTCTGGTTGGACCTTGGTGCAGGTGCTGCATTACAAA
TACCAATTTGCTATGCAAAATGGCTTATAGGTTTAAATGGTATTGGAGTTACACAGAATGTTCTCTATGAGAACCAAAAATGATTGCC
AACCAATTTAATAGTGTCTATTGGCAAAAATCAAGACTCACTTTCTCCACAGCAAGTGCCTTGGAAAACCTCAAGATGTGGTCAA
CCATAATGCACAAGCTTTAAACACGCTTGTTAAACAACCTTAGCTCCAAATTTGGTGCATTTCAAGTGTTTTAAATGATATCTTTTC
ACGCTTGTACAAAAGTTGAGGCTGAAGTGCAAATTGATAGGTTGATCACAGGCAGACTGCAGAGCCTCCAGACATACGTGACCCAG
CAGCTGATCAGAGCCGCCGAGATTAGAGCCTCTGCCAATCTGGCCGCCACCAAGATGTCTGAGTGTGTGCTGGGCCAGAGCAAGA
GAGTGGACTTTTGGCGCAAGGGCTACCACCTGATGAGCTTCCCTCAGCTGCCCCCTCAGGCGTGGTGTCTTCTGCACGTGACATAC
GTTCCCGCTCAAGAGAAGAAATTTACCACCGCTCCAGCCTCTGCCACGACGGCAAAGCCACTTTCTAGAGAAGGCGTGTTCG
TGTCCAACGGCACCCATTTGGTTCGTGACACAGCGGAATCTACGAGCCAGATCATACCACCGACAACCTTCTGTGTCTGG
CAACTGCGACGTGCTGATCGGCATTGTGAACAATACCGTGTACGACCCTCTGCAGCCGAGCTGGACAGCTTCAAAAGAGGAACCTG
GACAAGTACTTTAAGAACCACACAAGCCCGACGTGGACCTGGGCGATATCAGCGGAATCAATGCCAGCGTCTGTAACATCCAG
AAAGAGATCGACCGGCTGAACGAGGTGGCCAAGAATCTGAACGAGAGCCTGATCGACCTGCAAGAAGTGGGGAAGTACGAGCA
GTACATCAAGTGGCCCTGGTACATCTGGCTGGGCTTTATCGCCGACTGATTGCCATCGTGTGATGGTACAATCATGCTGTGTGCA
TGACCAGCTGCTGTAGCTGCCTGAAGGGCTGTTGTAGCTGTGGCAGCTGCTGCTAG
```

## 2. Monoclonal Antibody Production

Antibody sequences were extracted from deposited RCSB entries and codon optimized (using a human germline-aware codon optimization strategy), then synthesized as gene fragments and cloned into pTWIST transient expression vectors by Gibson assembly or restriction cloning (NotI, BamHI). Cloned plasmids were verified by sanger sequencing.

Expi293 cells were transfected with plasmids encoding for the heavy and light chain at 1µg/mL (i.e. 0.5µg/mL each) according to the manufacturer's instructions (ThermoFisher). Dense Expi293 cultures (day 5-7 post transfection) were

centrifuged at 300xg for 5 minutes to pellet the cells. Supernatant was filtered using Steriflip® 0.22 µm (Merck) filter units. Expi supernatant was directly loaded onto Protein G Agarose (Pierce) gravity columns, washed twice with PBS and eluted using Protein G Elution Buffer (Pierce). The eluted fractions were immediately neutralized with 1M TRIS-Buffer (pH = 8) to physiological pH. Absorption at 280 nm was quantified by Nanodrop™ 2000c to determine protein containing fractions. These fractions were then pooled and buffer exchanged using SnakeSkin™ dialysis tubing (10 MWCO, Pierce) followed by further dialysis and concentration using Amicon Ultra-4 10kDa centrifugal units (Merck).

### **3. AlphaFold2 Omicron Model**

AlphaFold2<sup>2</sup>, implemented in ColabFold<sup>3</sup>, was used to construct models of two overlapping Omicron spike fragments, with residues 1 to 698, (founder coordinates) and 590 to 1147, using “Templates=true”, and without Amber relaxation. The amino acid sequence used was identical to that which we cloned into our PSV plasmid. These two fragment models were pieced together using their overlap (in Chimera 1.15), and this was found to adopt the conformation that matched the “RBD-down” protomer in PDB: 7MJJ<sup>4</sup>, which was used to contextualize the visualization in figure 1.

### **4. Monoclonal Antibody Escape Mutations**

The RBD from the AlphaFold2 model was docked into a crystal complex for each mAb. Sites that were mutated in Omicron, and proximal to the mAb/RBD interface, were selected, and cross-referenced with deep mutational scanning data, and visualized in dms-view<sup>5</sup>.

PDBs used: 6XDG<sup>6</sup> (REGN-10933 and REGN-10987), 7KMG<sup>7</sup> (LY-CoV555) 7C01<sup>8</sup> (LY-CoV016), 6WPS<sup>9</sup> (S309).

Deep Mutational Scanning data from:

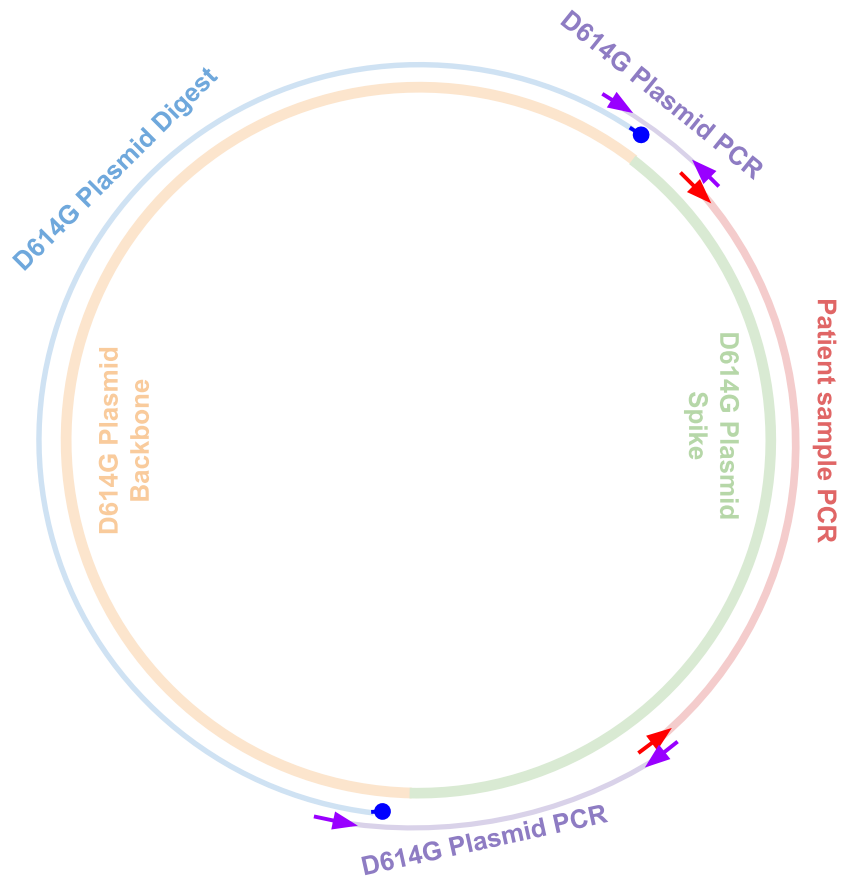
[https://jbloomlab.github.io/SARS-CoV-2-RBD\\_MAP\\_clinical\\_Abs/](https://jbloomlab.github.io/SARS-CoV-2-RBD_MAP_clinical_Abs/)<sup>10</sup>

[https://jbloomlab.github.io/SARS-CoV-2-RBD\\_MAP\\_LY-CoV555/](https://jbloomlab.github.io/SARS-CoV-2-RBD_MAP_LY-CoV555/)<sup>11</sup>

[https://jbloomlab.github.io/SARS-CoV-2-RBD\\_MAP\\_Vir\\_mAbs/](https://jbloomlab.github.io/SARS-CoV-2-RBD_MAP_Vir_mAbs/)<sup>12</sup>

**Supplementary Figures**

**A**

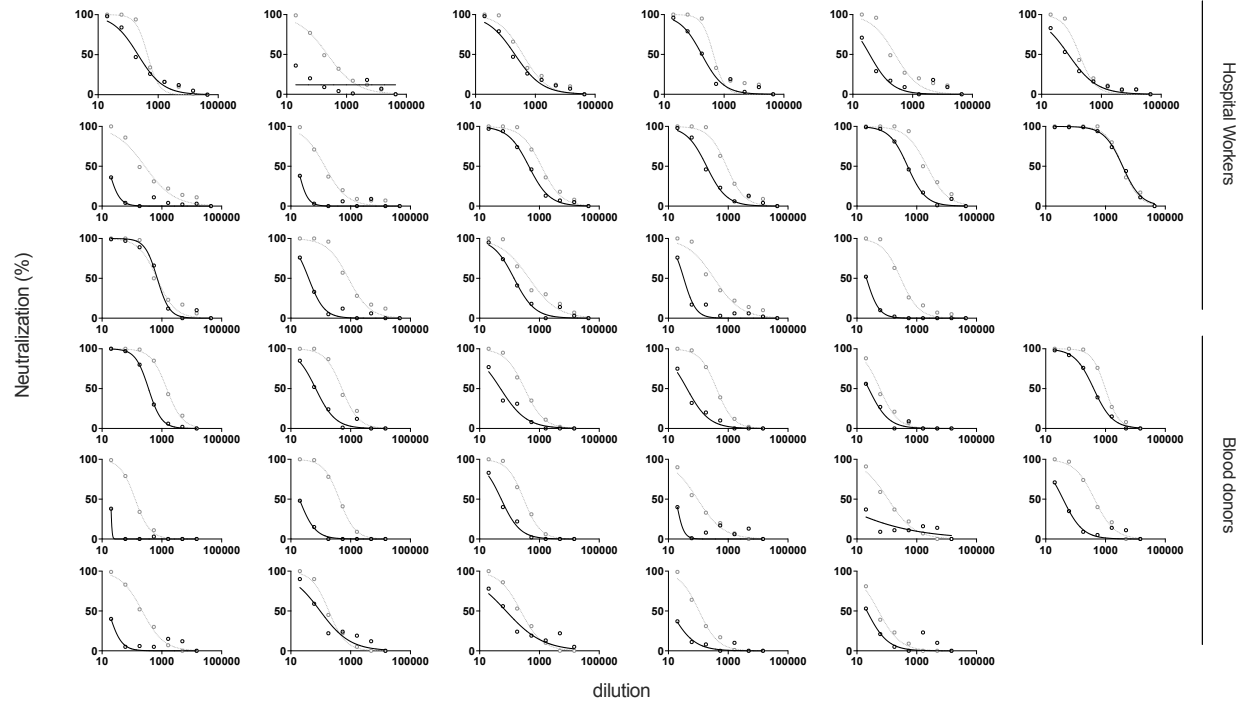


**B**

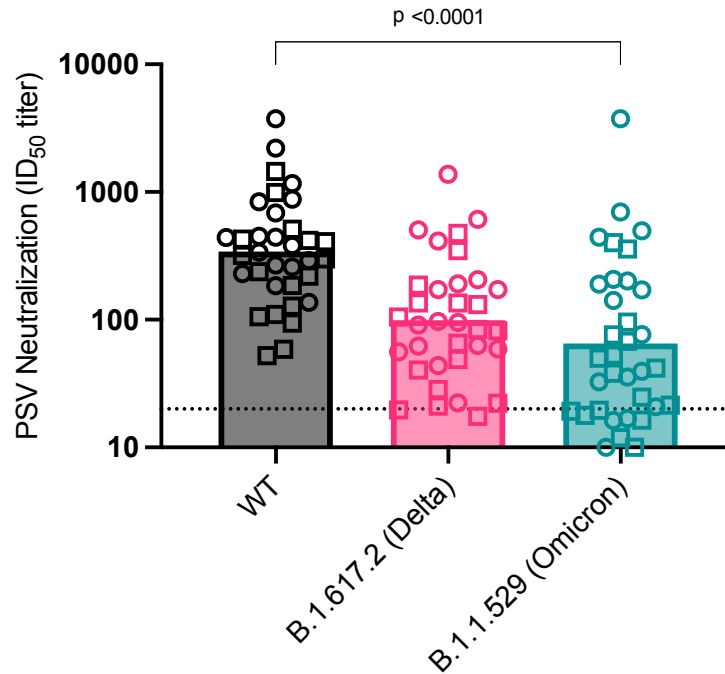
```

Primer: FWD_N_term_sample      5'- caaggtgttcagatccttcagttttacattcaactc - 3'
Omicron Sample tttattaccctgacaaaagttttcagatccttcagttttacattcaactcaggacttggt
D614G Plasmid gtactacccgacaaggtgttcagatccagcgtgctgcactctaccaggacctggt
Primer: REV_N_term_plasmid (Rev Comp) 3'- ccgacaaggtgttcagatccttcagttttacattca - 5'
  
```

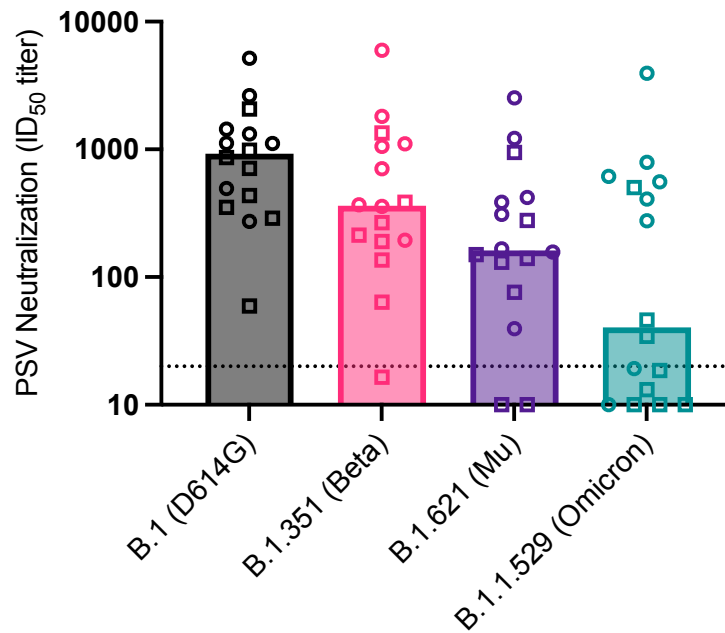
**Supplementary Figure 1. Cloning strategy.** **A** depicts the 4-fragment gibson assembly, combining a digested D614G plasmid backbone, two PCR fragments that incorporate the N terminus and C terminus of the codon optimized D614G spike, and the Omicron spike amplified from a patient sample. **B** shows an example of the junction between the codon optimized D614G plasmid and the Omicron sample sequence. Differences between codon optimized D614G and codon native Omicron are in red, and a coincidentally long region of nucleotide identity (**bold**) was exploited to ensure i) sufficient 3' identity for PCR amplification, ii) sufficient 5' overhangs for gibson assembly, and iii) primer lengths less than or equal to 35bp, which was required for overnight synthesis.



**Supplementary Figure 2. Neutralization curves.** Neutralization curves for 17 sera each from the HW and BD cohorts against WT (grey) and Omicron/B.1.1.529 (black).

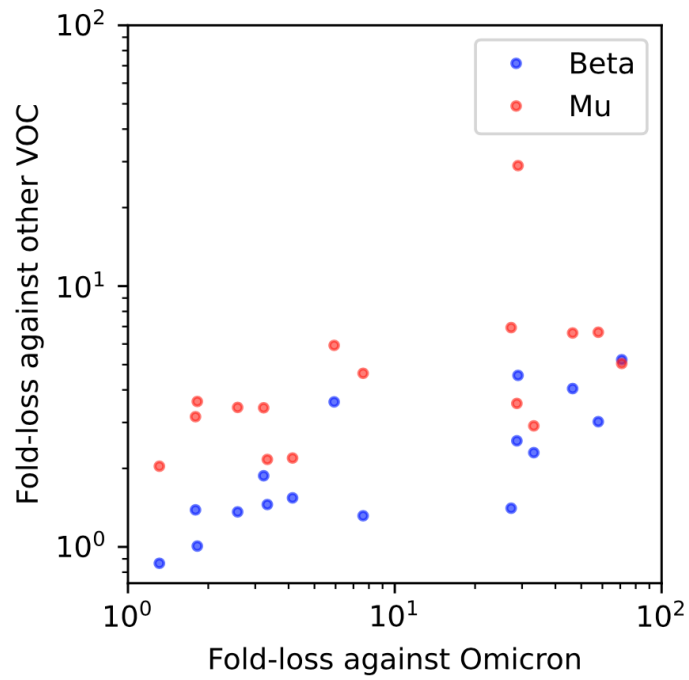


**Supplementary Figure 3. Neutralizing activity compared to Delta.** Neutralizing activity of sera from blood donors (BD) (squares) and Hospital Workers (HW) (circles) against WT, Delta, and Omicron.



**Supplementary Figure 4. Neutralizing activity compared to Beta and Mu.** Neutralizing activity of sera from a subset of BD (squares) and HW (circles) against B.1, Beta, Mu, and Omicron, from an independent assay replicate. Sample selection was biased towards samples that showed extreme maintenance or loss against Omicron. For the subset of samples included in both runs, Omicron titers were reproducible ( $\rho = 0.96$ , calculated from ID50s in the log domain).





**Supplementary Figure 5. Correlations.** For the subset of samples run against D614G, Omicron, Beta, and Mu, the fold-loss against Omicron (defined as D614G IC50/Omicron ID50) was more strongly correlated with fold-loss against Beta ( $\rho = 0.78$ , log domain) than Mu ( $\rho = 0.57$ , log domain).

## **Supplementary Tables**

**Supplementary Table 1.** List of mutations in the Omicron spike evaluated here, relative to Wu-Hu-1.

A67V  
H69-  
V70-  
T95I  
G142D  
V143-  
Y144-  
Y145-  
N211-  
L212I  
+214EPE  
G339D  
S371L  
S373P  
S375F  
K417N  
N440K  
G446S  
S477N  
T478K  
E484A  
Q493R  
G496S  
Q498R  
N501Y  
Y505H  
T547K  
D614G  
H655Y  
N679K  
P681H  
N764K  
D796Y  
N856K  
Q954H  
N969K  
L981F

**Supplementary Table 2.** Neutralizing ID<sub>50</sub> titers for pooled vaccine standard reagents.

	Founder ID <sub>50</sub>	Delta ID <sub>50</sub>	Omicron ID <sub>50</sub>
Pfizer	415	155	<20
Moderna	321	143	<20
J&J	385	178	57

**Supplementary Table 3. Heterogeneity in fold-changes.** Table shows statistics for the heterogeneity in the difference in  $\log_{10}$  neutralization titers (which is the logarithm of the Omicron/WT fold-change). The BD and HW groups have similar standard deviations, indicating that the degree of heterogeneity is similar between these groups. Also shown are Shapiro-Wilk test statistics and P values for the BD and HW cohort, failing to reject the null hypothesis that these are normally distributed, indicating that the fold changes themselves are consistent with a log-normal distribution.

	BD	HW
N	40	17
Mean	0.9152	0.675
Std. Deviation	0.411	0.4382
Lower 95% CI of mean	0.7838	0.4497
Upper 95% CI of mean	1.047	0.9003
Shapiro-Wilk W	0.9895	0.9476
Shapiro-Wilk P value	0.9676	0.4202

## References

- 1 Freed N, Silander O. SARS-CoV2 genome sequencing protocol (1200bp amplicon ‘midnight’ primer set, using Nanopore Rapid kit). 2021; published online July 29. <https://www.protocols.io/view/sars-cov2-genome-sequencing-protocol-1200bp-amplic-bwyppfvn> (accessed Dec 9, 2021).
- 2 Jumper J, Evans R, Pritzel A, *et al.* Highly accurate protein structure prediction with AlphaFold. *Nature* 2021; published online July 15. DOI:10.1038/s41586-021-03819-2.
- 3 Ovchinnikov S, Mirdita M, Steinegger M. ColabFold - Making Protein folding accessible to all via Google Colab. 2021 DOI:10.5281/zenodo.5123297.
- 4 Zhu X, Mannar D, Srivastava SS, *et al.* Cryo-electron microscopy structures of the N501Y SARS-CoV-2 spike protein in complex with ACE2 and 2 potent neutralizing antibodies. *PLoS Biol* 2021; **19**: e3001237.
- 5 Hilton SK, Huddleston J, Black A, *et al.* dms-view: Interactive visualization tool for deep mutational scanning data. *J Open Source Softw* 2020; **5**. DOI:10.21105/joss.02353.
- 6 Hansen J, Baum A, Pascal KE, *et al.* Studies in humanized mice and convalescent humans yield a SARS-CoV-2 antibody cocktail. *Science* 2020; **369**: 1010–4.
- 7 Jones BE, Brown-Augsburger PL, Corbett KS, *et al.* The neutralizing antibody, LY-CoV555, protects against SARS-CoV-2 infection in nonhuman primates. *Sci Transl Med* 2021; **13**. DOI:10.1126/scitranslmed.abf1906.
- 8 Shi R, Shan C, Duan X, *et al.* A human neutralizing antibody targets the receptor-binding site of SARS-CoV-2. *Nature* 2020; **584**: 120–4.
- 9 Pinto D, Park Y-J, Beltramello M, *et al.* Cross-neutralization of SARS-CoV-2 by a human monoclonal SARS-CoV antibody. *Nature* 2020; **583**: 290–5.
- 10 Starr TN, Greaney AJ, Addetia A, *et al.* Prospective mapping of viral mutations that escape antibodies used to treat COVID-19. *Science* 2021; **371**: 850–4.
- 11 Starr TN, Greaney AJ, Dingens AS, Bloom JD. Complete map of SARS-CoV-2 RBD mutations that escape the monoclonal antibody LY-CoV555 and its cocktail with LY-CoV016. *Cell Rep Med* 2021; **2**: 100255.
- 12 Starr TN, Czudnochowski N, Liu Z, *et al.* SARS-CoV-2 RBD antibodies that maximize breadth and resistance to escape. *Nature* 2021; **597**: 97–102.